Electronic Supplementary Material (ESI) for Analyst.

Supplementary Mateials

Preparation and application of high-brightness red carbon quantum dots for pH and oxidized L-glutathione dual response

Yuwei Du, [a,c] Lei Cao, [a,c] Xinlu Li, [a,c] TongTong Zhu, [a,c] Ruhong Yan, [*,b,c] Wen-Fei Dong [*,a, c] and Li Li [*,a,c,d]

a. School of Biomedical Engineering (Suzhou), Division of Life Sciences and Medicine, University of Science and Technology of China, Hefei 230026, China.

b. Department of Clinical Laboratory, Suzhou Hospital, Affiliated Hospital of Medical School, Nanjing University, Suzhou, 215153, China.

E-mail: yrhzl@hotmail.com

c. CAS Key Laboratory of Biomedical Diagnostics, Suzhou Institute of Biomedical Engineering and Technology, Chinese Academy of Science (CAS), Suzhou, 215163, China.

E-mail: wenfeidong@sibet.ac.cn

d. Jinan Guokeyigong Science and Technology Development Co., Ltd, Jinan, 250104, China.

E-mail: lil@sibet.ac.cn

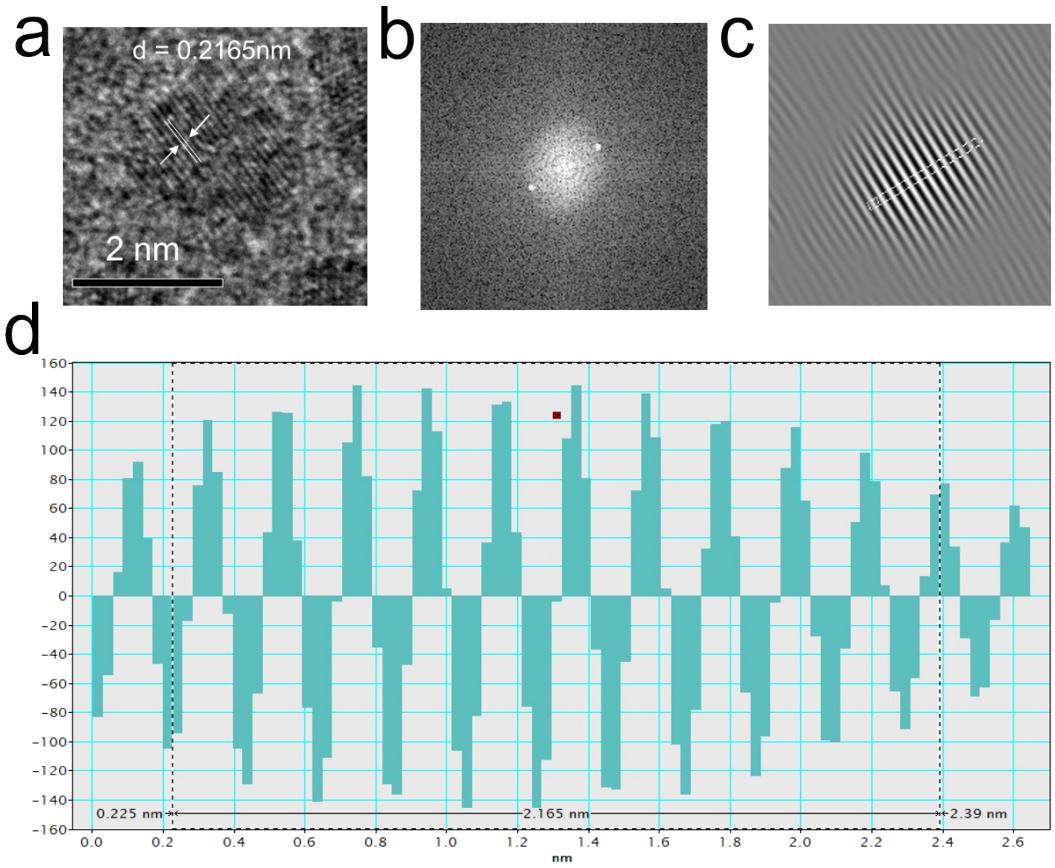

Figure S1. (a) HR-TEM image of the R-CDs. FFT pattern (b) and IFFT pattern (c) of the R-CDs. (d) The calculation of lattice d-spacing of the R-CDs (0.2165nm).

Table S1. The elemental composition and functional group percentages of the R-CDs measured by XPS.

Atom	Atomic %
C	63.04
N	3.16
O	27.15
Br	3.28

Name	Functional group	Area (%)
C1 s	C-C/C=C	95.26
	C-N/C-O	4.74
N1 s	Pyridinic N	8.95
	Pyrrolic N	56.29
	Graphitic N	34.76
O1 s	C=O	37.44
	C-O	62.56
Br 3d	H-Br $3d_{3/2}$	44.51
	C-Br $3d_{5/2}$	30.98
	C-Br $3d_{3/2}$	24.51

Table S2. The comparison of different red-emitting carbon dots synthesis precursors, synthesis method, application, the optimal emission wavelength (λ_{em}), and the absolute quantum yield. The absolute quantum yield of the R-CDs is 11.93%.

Precursors	Synthetic method	Application	λ_{em}	Quantum yield	Ref.
Citric acid, urea	hydrothermal	fluorescence mechanism	602 nm	4.00%	[1]
2,5-Diamino-benzenesulfonic acid, 4-aminophenylboronic acid hydrochloride	hydrothermal	Fe^{3+} detection, cell	600 nm	5.44%	[2]
Citric acid, ethylene glycol	hydrothermal	fluorescence mechanism	610 nm	6%	[3]
Alizarin carmine	hydrothermal	GSH detection, cell	642 nm	6.3%	[4]
Citric acid, urea	solvothermal	LED	600 nm	7.40%	[5]
Citric acid, urea	solvothermal	cell	658 nm	9.8%	[6]
p-Phenylenediamine	solvothermal	cell	620 nm	3-10.4%	[7]
1,2-Diamino-4-bromobenzene	solvothermal	cell	662 nm	11.93%	This work

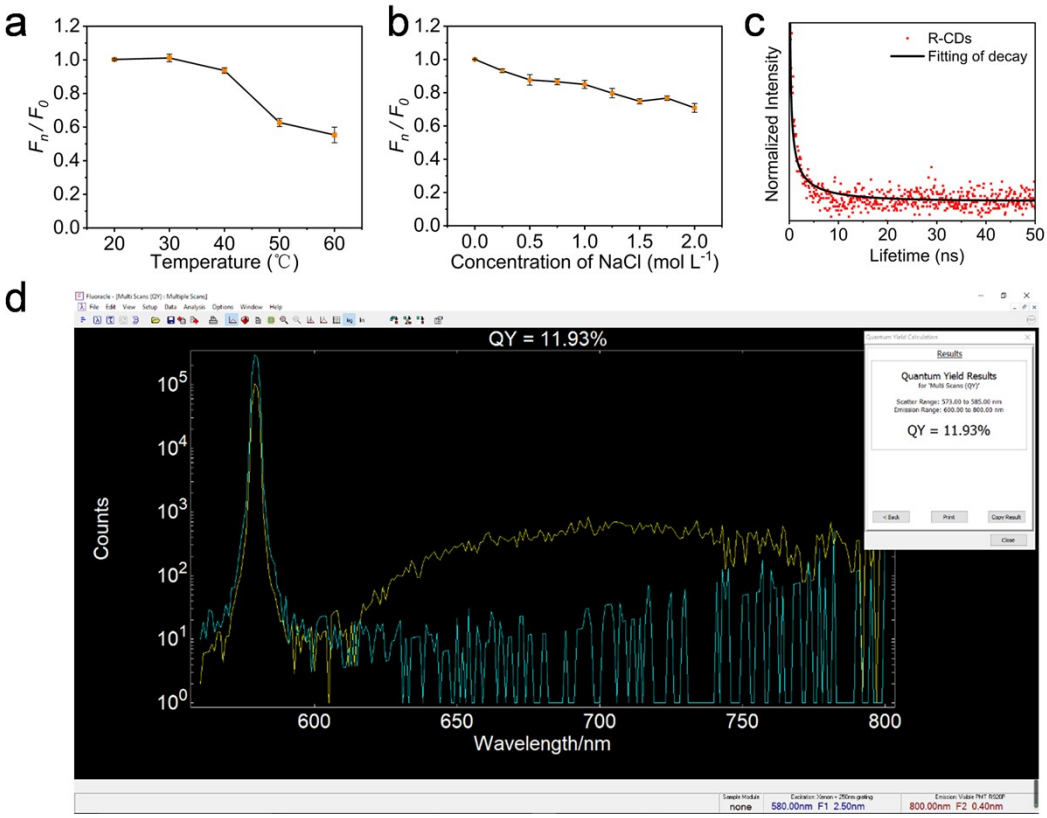

Figure S2. (a) Effects of different temperature on the fluorescence intensity of the R-CDs. F_0 and F_n are the fluorescence intensities of the R-CDs at 20℃ and different temperature. (b) Effects of ionic strengths on the fluorescence intensity of the R-CDs. F_0 and F_n are the fluorescence intensities of the R-CDs in 0 mol L^{-1} and different concentrations of NaCl solution. (c) The fluorescence lifetime of the R-CDs. (λ_{ex} = 580 nm). (d) The absolute quantum yield of the R-CDs is as high as 11.93%.

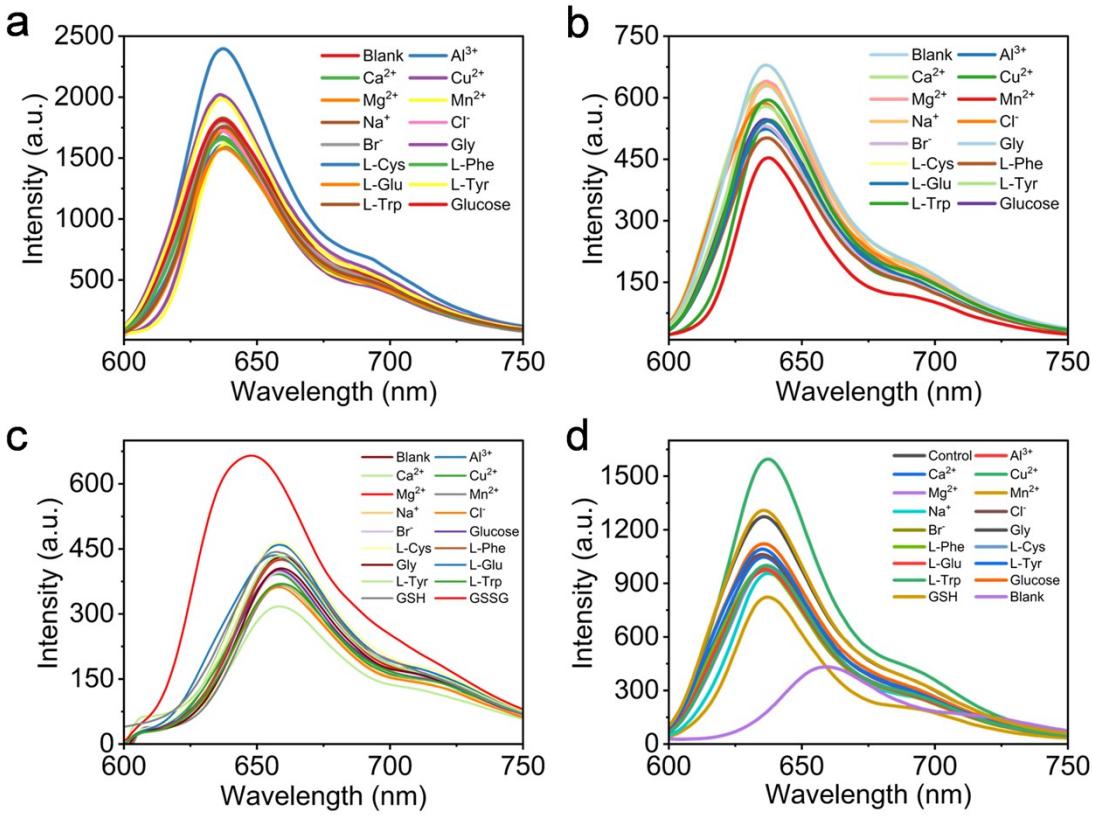

Figure S3. The Fluorescence spectra of the R-CDs with the addition of 0.1mM of different interfering substances (Al^{3+}, Ca^{2+}、Cu^{2+}, Mg^{2+}、Mn^{2+}, Na^{+}, Cl^{-}, Br^{-}、Glucose，L-Cys、L-Phe、Gly、L-Glu、L-Tyr、L-Trp、GSH) at pH 2.0 (a) and pH 7.0 (b). (c) The fluorescence spectra of the R-CDs with the addition of 0.1mM of different interfering substances. (d) The fluorescence spectra of the R-CDs with the addition of 0.1mM of different interfering substances or the interfering substances and GSSG.

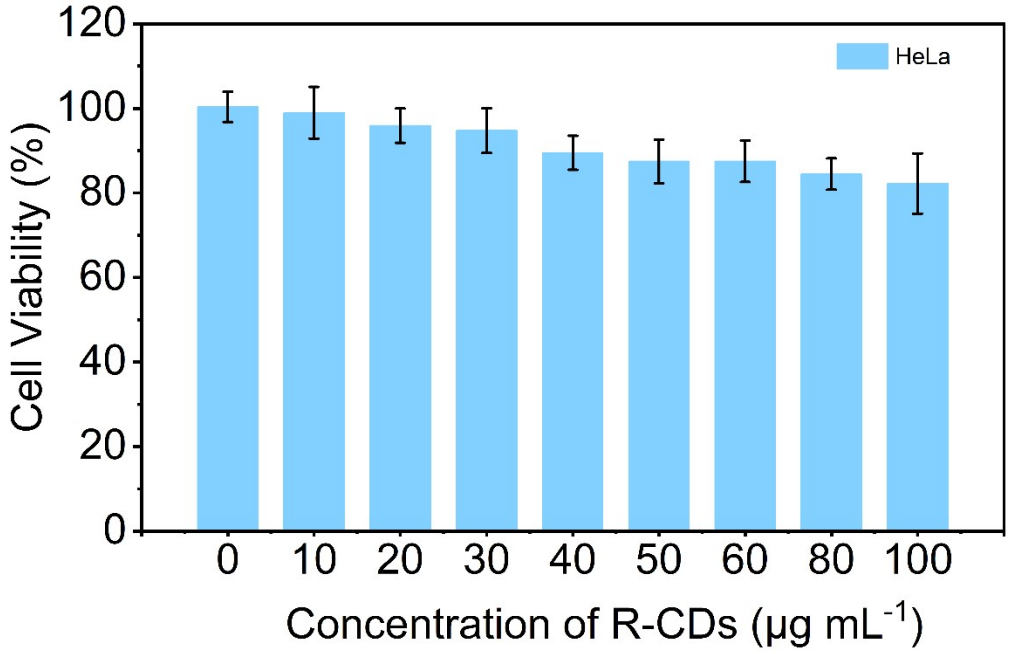

Figure S4. Cytotoxicity assays of the R-CDs against HeLa cells.

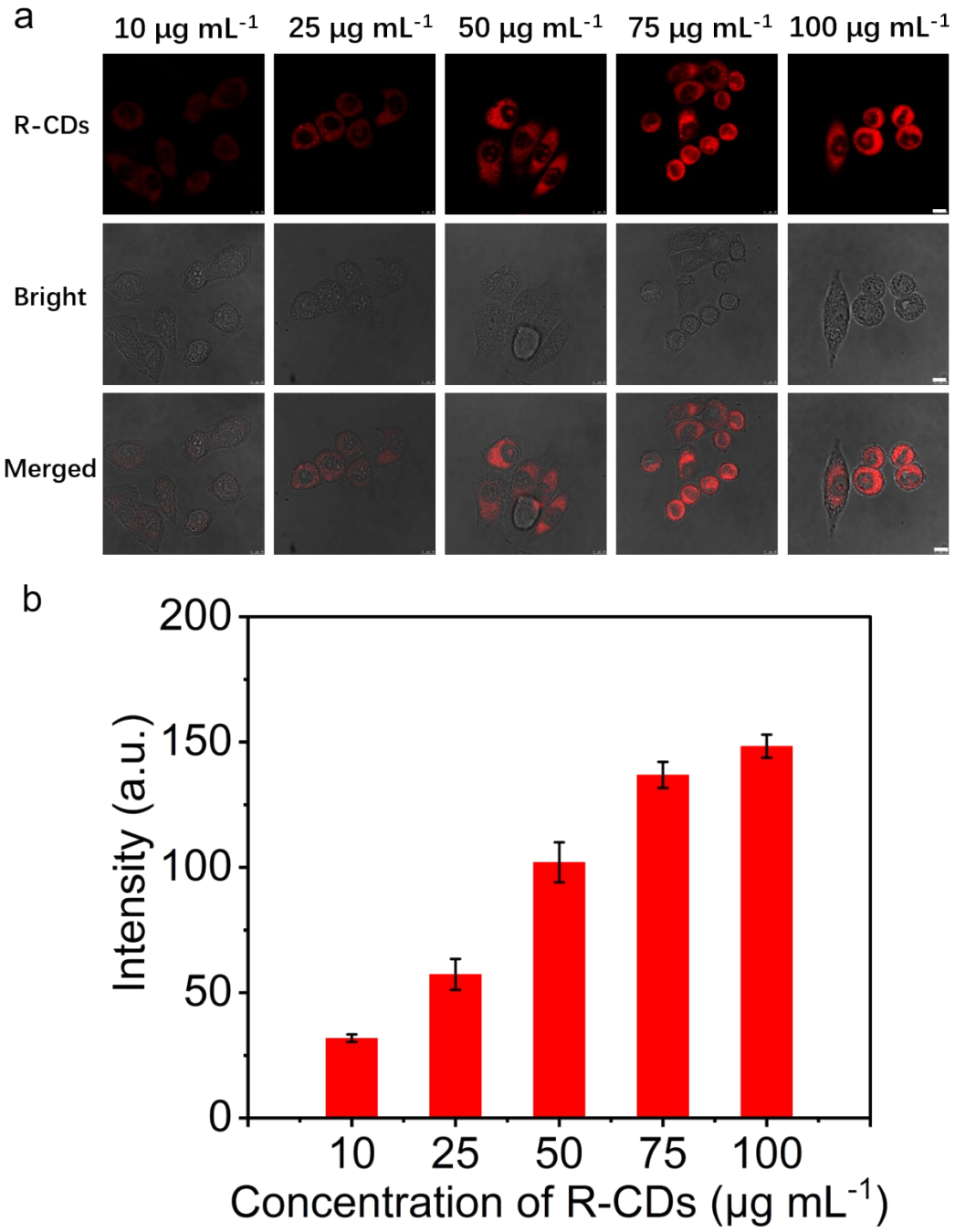

Figure S5. (a) The laser scanning confocal microscope images of HeLa cells co-incubated with the R-CDs at different concentrations (5, 10, 15, and 20 μg mL^{-1}). (b) The corresponding average fluorescence intensities from the images in (a). The scale bar is 10 μm.

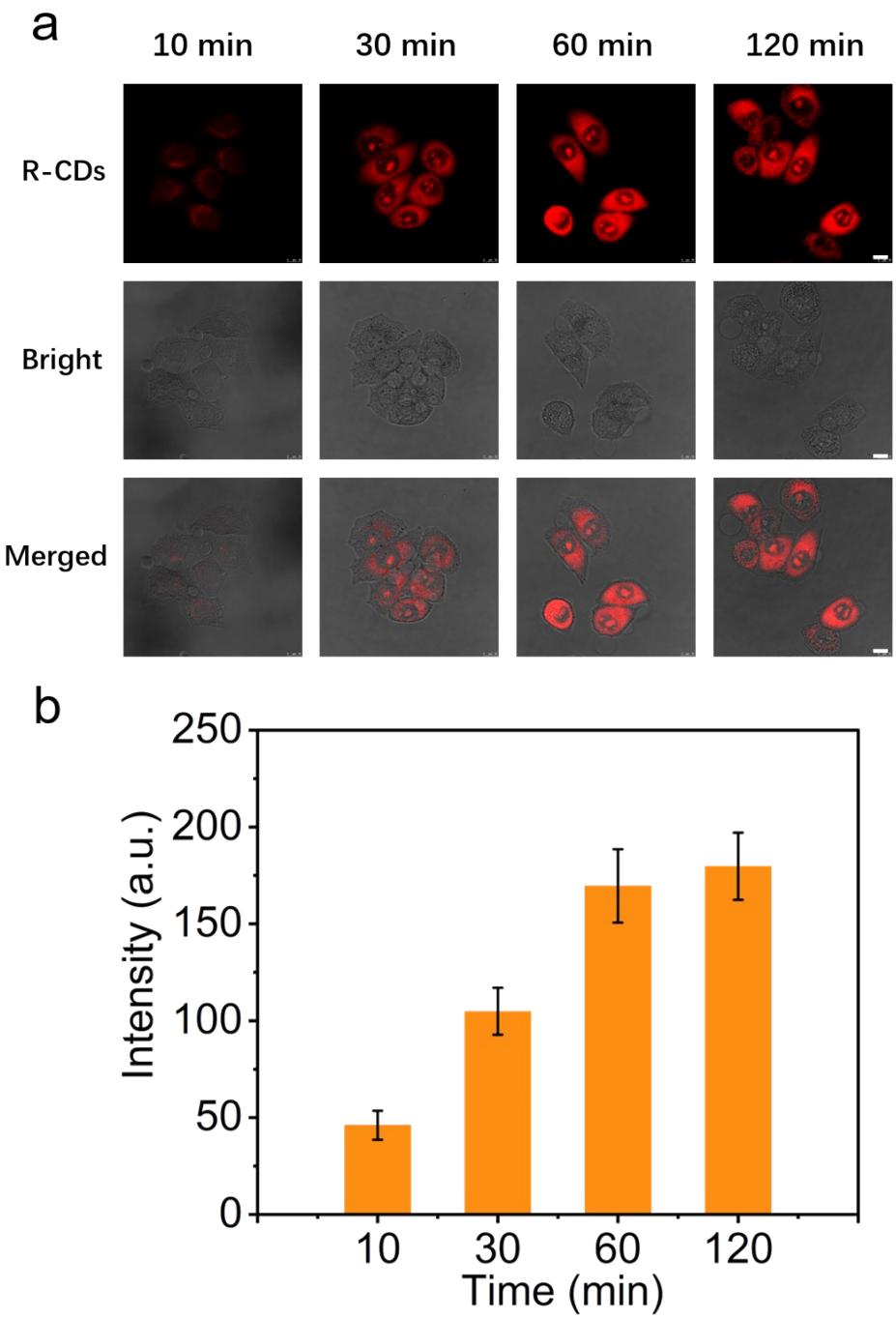

Figure S6. (a) The laser scanning confocal microscope images of HeLa cells co-incubated with the R-CDs (75 μg mL^{-1}) for 10, 30, 60, and 120 min. (b) The corresponding average fluorescence intensities from the images in (a). The scale bar is 10 μm.

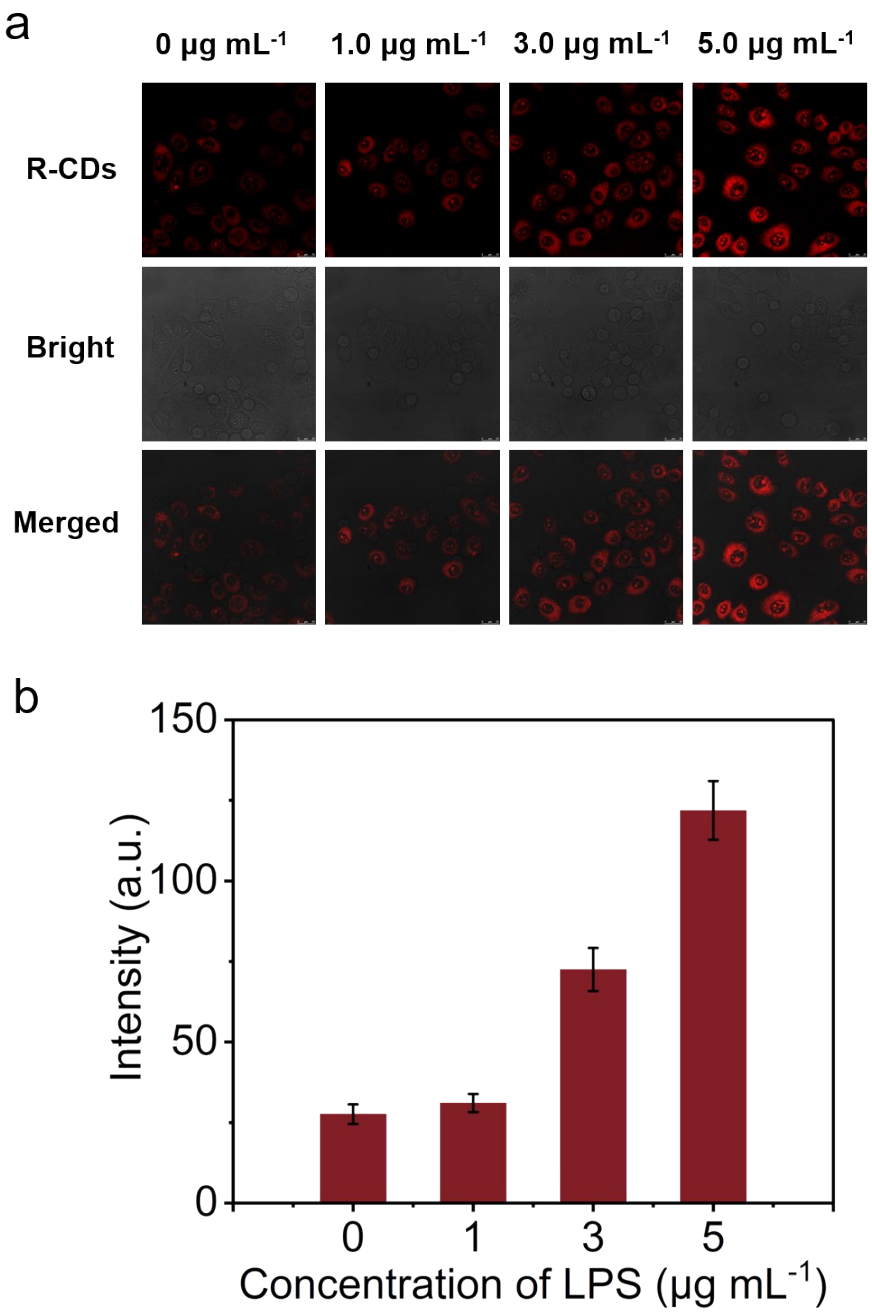

Figure S7. (a) The laser scanning confocal microscope images of HeLa cells co-incubated with the R-CDs (75 μg mL^{-1}) treated with different concentration of LPS (0, 1, 3, and 5 μg mL^{-1}). (b) The corresponding average fluorescence intensities from the images in (a). The scale bar is 25 μm.

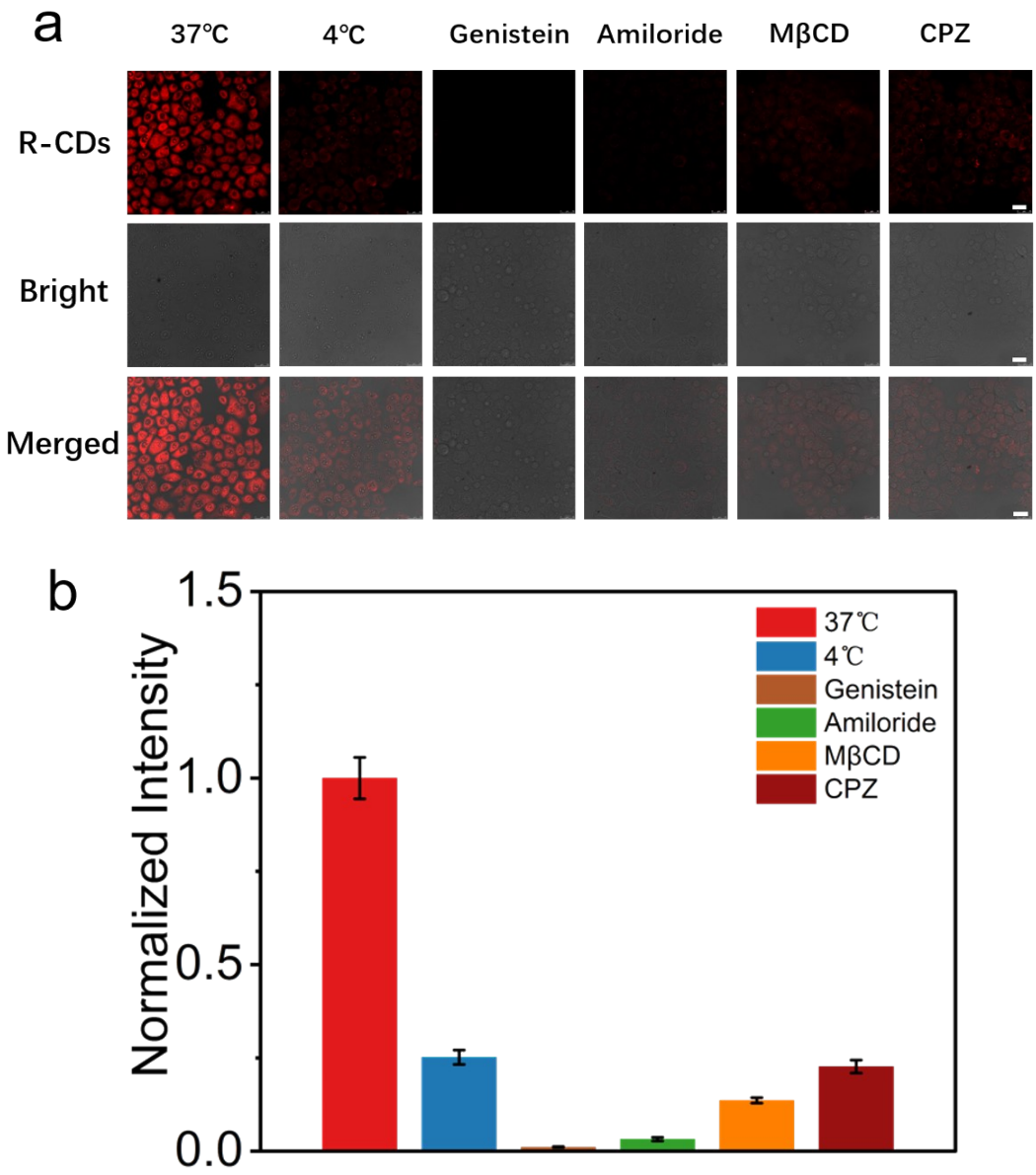

Figure S8. (a) Laser scanning confocal microscope images of HeLa cells without or with treatments of inhibitors (4℃, 50 μg mL^{-1} Genistein, 10 μg mL^{-1} Amiloride, 5 μg mL^{-1} MβCD, 5 μg mL^{-1} CPZ). (b) The corresponding average fluorescence intensities from the 6 images in (a). The scale bar is 25 μm.

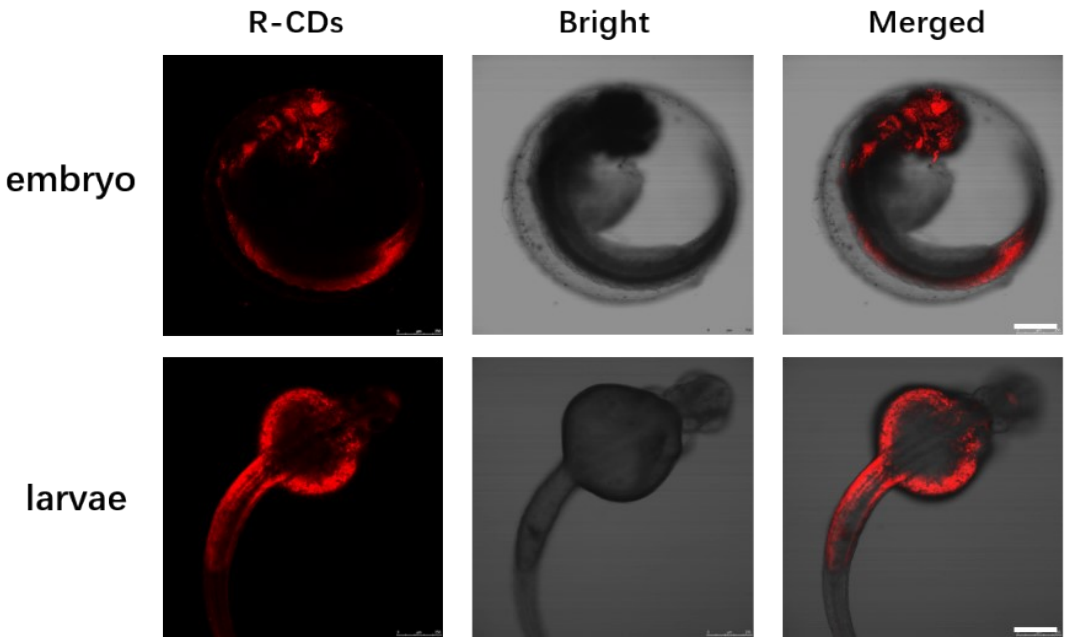

Figure S9. Laser scanning confocal microscope images of living zebrafish embryo and zebrafish larvae co-incubated with the R-CDs (75 μg mL^{-1}). The scale bar is 0.25 mm.

References

1 K. Holá, M. Sudolská, S. Kalytchuk, D. Nachtigallová, A. L. Rogach, M. Otyepka and R. Zbořil, *ACS Nano*, 2017, **11**, 12402-12410.

2 Y. Liu, W. Duan, W. Song, J. Liu, C. Ren, J. Wu, D. Liu and H. Chen, *ACS Appl Mater Interfaces*, 2017, **9**, 12663-12672.

3 L. Bao, C. Liu, Z. L. Zhang and D. W. Pang, *Adv Mater*, 2015, **27**, 1663-1667.

4 L. Li, L. Shi, J. Jia, O. Eltayeb, W. Lu, Y. Tang, C. Dong and S. Shuang, *ACS Appl Mater Interfaces*, 2020, **12**, 18250-18257.

5 X. Miao, D. Qu, D. Yang, B. Nie, Y. Zhao, H. Fan and Z. Sun, *Adv Mater*, 2018, **30**, 1704740.

6 L. Jiang, H. Ding, M. Xu, X. Hu, S. Li, M. Zhang, Q. Zhang, Q. Wang, S. Lu, Y. Tian and H. Bi, *Small*, 2020, **16**, e2000680.

7 H. Wang, J. Wei, C. Zhang, Y. Zhang, Y. Zhang, L. Li, C. Yu, P. Zhang and J. Chen, *Chinese Chemical Letters*, 2020, **31**, 759-763.